IEEE Access
Multidisciplinary | Rapid Review | Open Access Journal

Received December 31, 2019, accepted January 19, 2020, date of publication February 3, 2020, date of current version February 14, 2020.

Digital Object Identifier 10.1109/ACCESS.2020.2971262

Dual-Beam Leaky-Wave Antenna Array With Capability of Fixed-Frequency Beam Switching

XIAOWEN LI, JUNHONG WANG, (Senior Member, IEEE), ZHENG LI, (Member, IEEE), YUJIAN LI, (Member, IEEE), MEIE CHEN, AND ZHAN ZHANG

Key Laboratory of All Optical Network and Advanced Telecommunication Network of MOE, Beijing Jiaotong University, Beijing 100044, China
Institute of Lightwave Technology, Beijing Jiaotong University, Beijing 100044, China

Corresponding author: Junhong Wang (wangjunh@bjtu.edu.cn)

This work was supported by the National Nature Science Foundation of China under Grant 61871025.

ABSTRACT A novel fixed-frequency beam switchable dual-beam antenna array is presented, which consists five dual-beam leaky-wave antenna (LWA) elements designed on substrate integrated waveguide (SIW) and integrated together on a common substrate. The LWAs work on fundamental wave and -1th spatial harmonic wave simultaneously and excite two symmetrical radiation beams in forward and backward direction respectively. In order to realize beam switching, three voltage-driven radio frequency chip switches (CSW-RFs) are used and integrated behind the antenna aperture. Since the periodic slot in LWA causes open stopband at the operating frequency, so the staggered radius amplification of local vias in the via walls of SIW is performed to suppress the open stopband. In addition, electromagnetic band-gap (EBG) structures, capable of reducing coupling between neighboring antenna elements, are embedded in between LWAs. The proposed dual-beam antenna array with beam switching capability between ±35, ±45, ±55, ±65 and ±75 degrees at 28 GHz are simulated, fabricated and measured. Both analysis and measurement results show that the proposed antenna array exhibits an excellent performance, which can be used in fixed-frequency beam-switching millimeter wave communication.

INDEX TERMS Leaky wave antenna (LWA), dual-beam, open stopband suppression, beam switching, radio frequency chip switch.

I. INTRODUCTION

As one typical type of traveling-wave antenna, leaky-wave antenna (LWA) based on substrate integrated waveguide (SIW) exhibits excellent advantages, such as high directivity, low profile and inherent frequency scanning capability [1], [2], and has been applied in various communication systems, especially for the beam-steering or pattern-reconfigurable applications [3]–[5], [6]–[9]. As we know, dual-beam scanning antennas, which build wireless links with two users or devices simultaneously, can provide flexible and diversified beam coverage [10]–[21].

As early as 1997, a dual-beam microstrip leaky-wave antenna (MLWA) using central fed CPW to excite the high-order mode is proposed, which makes energy leak in two directions to form dual beam [10]. Dual-beam radiations are also realized by exciting high-order mode of MLWA [11], [12], and making use of advantage of feeding configurations [13]–[15]. Recently, frequency dual-beam scanning MLWA and dielectric grating antenna are studied [16], [17], which use two spatial harmonics ($m = 1$ and 2) to generate dual-beam patterns. In addition, active devices are also used in generation of dual-beam radiation [18], [19], which improve the dual-beam frequency scanning properties. For the SIW based dual-beam LWA, a few works can be found. In [20], a dual-beam SIW LWA is proposed based on the orthogonal excitation of TE_{10} and TE_{01} modes which radiate through the top wall and lateral wall of waveguide respectively, so two radiation beams are generated. However, the two beams of this antenna cannot scan and the gain difference between them is more than 3 dB. In [21], the original metal vias on both side walls of SIW are replaced by metal blocks with large spacing, so dual-direction energy leakage is generated and two beams in H-plane are excited. This antenna

The associate editor coordinating the review of this manuscript and approving it for publication was Raheel M. Hashmi.

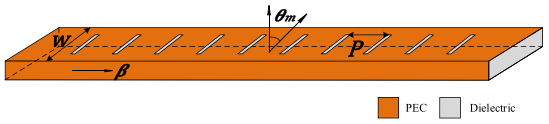

FIGURE 1. Basic structure of the proposed SIW LWA.

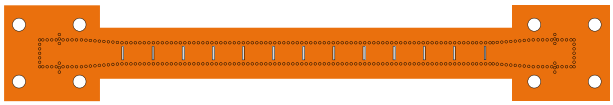

FIGURE 2. Configuration of the periodically slotted leaky rectangular waveguide.

structure is simple and is capable of dual-beam scanning by changing frequency, but the gain of it is not clear. Although these dual-beam antennas show outstanding capabilities in frequency beam-scanning, in some applications, it is desired to make beam scanning at a certain frequency [6]. To the best of our knowledge, few works concern about fixed-frequency dual-beam scanning SIW LWA can be found so far.

In this paper, a novel method to achieve dual-beam SIW leaky-wave array by employing co-radiation of the fundamental wave and -1th spatial harmonic wave is presented. The fixed-frequency beam scanning is realized by switching the excitation between feed ports of the array elements. Traditionally, switching between feed ports depends on manual operation [22], [23]. Here, we adopt three voltage-driven CSW-RF switches to select the feed port and integrated them on the back of array, so the beam scanning can be realized by changing supply voltages. Moreover, the open stopband issue, a common problem with SIW LWA when beam scan to the broadside direction, is also overcome by a new open stopband suppression approach.

This paper is organized as follows. In Section II, theory and method of the design of dual-beam SIW LWA is introduced. In Section III, design procedures of the dual-beam LWA elements and array including the suppression of open stopband are given. Simulated and measured results of the antenna array are given in Section IV. Realization of beam switching by integrating CSW-RF switches network are given in Section V. Conclusions are drawn in Section VI.

II. THEORY AND FORMULAS

The proposed LWA, as shown in Fig. 1, is working on fundamental wave ($m = 0$) and -1th spatial harmonic wave ($m = -1$) simultaneously, and excites two radiation beams in forward and backward direction respectively. By selecting structure parameters properly, the LWA can generate a symmetrical dual-beam radiation pattern.

As we know, a uniform slow wave structure cannot produce radiation, so periodic slots are usually introduced to modulate the guiding structure and generate infinite number of spatial harmonic waves with different wave numbers. Some of them have wave numbers less than that of free space, these harmonic waves can leak away and produce radiations [24]. Theoretically, the SIW LWA with periodic slots has similar properties as those of periodically slotted rectangular waveguide whose configuration is shown in Fig. 2.

The radiation condition and beam angle of the mth harmonic are [25]

$$-1 < \sqrt{\varepsilon_g} + m\lambda_0/P < 1, \tag{1}$$

$$\theta_m = sin^{-1}(\sqrt{\varepsilon_g} + m\lambda_o/P), \tag{2}$$

where λ_0 is the wavelength in free space, P is the period of slots, and ε_g is an equivalent dielectric constant of the leaky waveguide, its expression is [26]

$$\varepsilon_g = \varepsilon_r - (\frac{\lambda_0}{\lambda_c'})^2, \tag{3}$$

where ε_r is the dielectric constant of the material filled in the waveguide; λ_c' is the cut off wavelength of the fundamental mode in the leaky waveguide, and for a rectangular waveguide working at fundamental mode of TE_{10}, λ_c' is twice the width w of the dielectric filled rectangular waveguide.

From (2) and (3), the beam angles of the fundamental wave and -1th spatial harmonic can be obtained:

$$\theta_0 = \sin^{-1}[\sqrt{\varepsilon_r - (\frac{\lambda_0}{2w})^2}], \tag{4}$$

$$\theta_{-1} = \sin^{-1}[\sqrt{\varepsilon_r - (\frac{\lambda_0}{2w})^2} - \lambda_0/P]. \tag{5}$$

For the proposition of this paper, the condition of $\varepsilon_g < 1$ must be satisfied to guarantee the radiation from the fundamental wave ($m = 0$). According to equation (3), once the dielectric constant ε_r and frequency f are determined, the width of dielectric filled rectangular waveguide for $\varepsilon_g < 1$ should satisfy $w < \lambda_0/2(\sqrt{\varepsilon_r - 1})$. For the condition of working on TE_{10} mode of the waveguide, the operating wavelength λ should be larger than the cut-off wavelength of TE_{20} mode. So w can be expressed as $w < \lambda = \lambda_0/\sqrt{\varepsilon_r} < 2w$. Though above analysis, we can get the final range of w:

$$\lambda_0/(2\sqrt{\varepsilon_r}) < w < \min(\lambda_0/2(\sqrt{\varepsilon_r - 1}), \lambda_0/\sqrt{\varepsilon_r}). \tag{6}$$

By substituting (6) into (4), the corresponding range of radiation angle of fundamental wave can be obtained. By the way, from (4) we can also determine the value of w according to the radiation angle of fundamental wave.

In order to achieve the symmetrical dual-beam radiations, beam angle of the -1th spatial harmonic must satisfy

$$\theta_{-1} = -\theta_0. \tag{7}$$

From equation (5), we can see that equation (7) can be realized by properly selecting the slot period P. However, attention should also be paid to the suppression of radiation from higher harmonics. So the slot period P must satisfy

$$\begin{cases} \sqrt{\varepsilon_g} + m\lambda_0/P > 1, & m = 1, 2, 3\cdots \\ \sqrt{\varepsilon_g} + m\lambda_0/P < -1, & m = -2, -3, -4\cdots \end{cases} \tag{8}$$

Thus, the final conditions for the radiation of fundamental wave and -1st spatial harmonic are

$$\begin{cases} \dfrac{\lambda_0}{1+\sqrt{\varepsilon_g}} < P < \dfrac{\lambda_0}{1-\sqrt{\varepsilon_g}}, \varepsilon_g \le 1/9 \\ \dfrac{\lambda_0}{1+\sqrt{\varepsilon_g}} < P < \dfrac{2\lambda_0}{1+\sqrt{\varepsilon_g}}, 1/9 < \varepsilon_g \le 1 \end{cases} \tag{9}$$

Using equations (1) to (9), the equivalent width w and slot period P can be uniquely determined for producing the symmetrical dual-beam radiation pattern at the given frequency and dielectric constant.

III. DESIGN PROCEDURE

The SIW LWAs are designed on Rogers RT5880 substrate with thickness of $h = 1.575$ mm, permittivity of $\varepsilon_r = 2.2$ and loss tangent of 0.0009. The operating frequency is set to $f = 28$ GHz, which is the commercial frequency band put forward by the Third Generation Partnership Project (3GPP). According to equation (6) of section II, the final range of w is 3.6 mm $< w <$ 4.9 mm. In order to avoid the possible instability at the critical boundary, we select the value of w within 3.7 mm $< w <$ 4.8 mm. From (4), the theoretical beam angle range of fundamental wave is $19^\circ < \theta_0 < 77^\circ$. Using (7), the theoretical beam angle range of the -1th harmonic should be $-77^\circ < \theta_0 < -19^\circ$. Here, we give the design procedures by taking the LWA element with radiation beam angles of $\pm 35^\circ$ as an example.

A. DESIGN OF ANTENNA ELEMENT WITH RADIATION BEAMS POINTING TO $\pm 35^\circ$

The structure of SIW LWA is shown in Fig. 3, which can generate two beams by the fundamental wave and -1th spatial harmonic wave at 35 and -35 degrees respectively. In order to reduce the reflection, the width of SIW is linearly tapered at the ends. The antenna is fed by a Ka-band rectangular waveguide through a broadband rectangular waveguide to SIW transition [27]. The detail parameters of the antenna are listed in Table 1. As mentioned, the expected angle of fundamental wave radiation is 35°, the value of w calculated by (4) is 3.9 mm. From (3) we get $\varepsilon_g = 0.33$ and $\lambda_g = 18.65$ mm. Using (9), we find that P should be selected within 6.8 mm and 13.6 mm. As we know, SIW with width of a can be taken as a conventional dielectric-filled rectangular waveguide with an effective width of [26] $w = a - 1.08 \times d^2/s + 0.1 \times d^2/a$, where d is the diameter of the vias of SIW and s is the space between adjacent vias. Then, by choosing the conditions of $s/d = 1.7$ and $d/a = 0.125$ as used in [28], we get the values of a, s and d.

The next step is to realize the -1th spatial harmonic radiation with the beam angle of $\theta_{-1} = -35^\circ$ through selecting the period value of P by (5). We finally get $P = 9.3$ mm, which satisfies the condition of 6.8 mm $< P <$ 13.6 mm.

B. SUPPRESSION OF THE OPEN STOPBAND

From above analysis, we find that for a LWA with symmetrical dual-beam radiation pattern, the slots spacing is equal

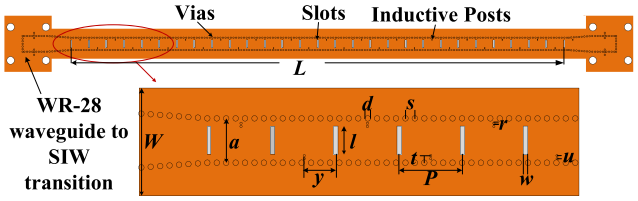

FIGURE 3. Structure of the SIW LWA element for ±35° radiation.

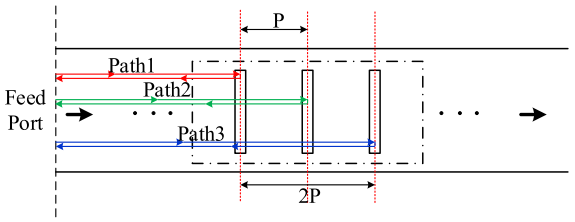

FIGURE 4. Propagation of electromagnetic wave.

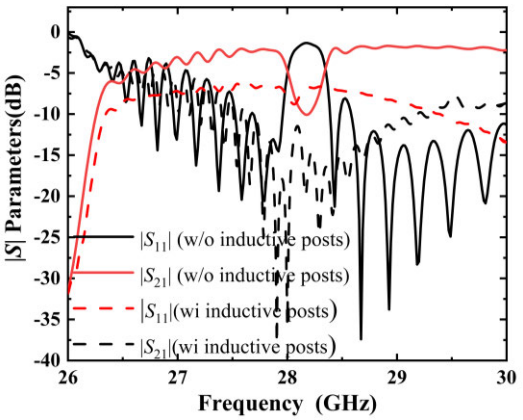

FIGURE 5. S-parameters of the SIW LWA with beam angles at ±35°.

to half of the waveguide wavelength $P = \lambda_g/2$. As described in Fig. 4, taking the wave paths of any three adjacent slots as an example, the corresponding phase difference is an integral multiple of 2π. This means that all the reflection waves caused by slots are superimposed in phase at the feed port. Therefore, the reflection coefficient will be rather large, which indicates that an open stopband will occur at the operating frequency of 28 GHz. Unlike the usual case of open stopband generation when beam pointing to broadside direction [29]–[31], the open stopband here occurs due to the interaction of two wave modes which generate two beams. Fig. 5 shows the open stopband in the simulated S-parameters of the antenna with beam angles of $\pm 35^\circ$.

In reference [29], by introducing inductive posts spaced by almost a quarter guided wavelength away from the adjacent slots to generate shunt inductances, the series inductances of the slots can be cancelled out, which results in suppression of the open stopband. Based on this principle, a set of cross-distributed inductive posts spaced $y = \lambda_g/4$ away

TABLE 1. Main parameters of antenna.

Parameter	Value(mm)	Parameter	Value(mm)	Parameter	Value(mm)	Parameter	Value(mm)
$L1$	260.4	$a1$	4.25	$p1$	9.3	λg_1	18.65
$L2$	212.8	$a2$	4.46	$p2$	7.6	λg_2	15.15
$L3$	182	$a3$	4.7	$p3$	6.5	λg_3	13.08
$L4$	165.2	$a4$	4.95	$p4$	5.9	λg_4	11.83
$L5$	154	$a5$	5.3	$p5$	5.5	λg_5	11.11
$w1$	0.35	$W1$	13.6	$dv1$	1	$pmin_1$	6.8
$w2$	0.45	$W2$	12	$dv2$	1.15	$pmin_2$	6.3
$w3$	0.5	$W3$	11.2	$dv3$	1.27	$pmin_3$	5.9
$w4$	0.5	$W4$	10.9	$dv4$	1.45	$pmin_4$	5.6
$w5$	0.45	$W5$	10.17	$dv5$	2.1	$pmin_5$	5.5
$l1$	3.2	$d1$	0.5	$s1$	0.9	$pmax_1$	13.6
$l2$	3	$d2$	0.6	$s2$	0.95	$pmax_2$	12.6
$l3$	3	$d3$	0.85	$s3$	1	$pmax_3$	11.8
$l4$	2.92	$d4$	0.75	$s4$	1.05	$pmax_4$	11.2
$l5$	3	$d5$	1.1	$s5$	1.1	$pmax_5$	11
r	0.15	$t1$	0.5	re	0.3	dp	5
u	0.025	eg_1	0.33 (wo unit)	ge	0.2		
eg_2	0.5 (wo unit)	eg_3	0.67 (wo unit)	we	0.78		
eg_4	0.82 (wo unit)	eg_5	0.93 (wo unit)	dx	10		

from the slots are introduced into the waveguide, as shown in Fig. 3, appropriate shunt inductances of these posts can obtain by adjusting their diameter r, relative distance t and adjacent distance u [29]. Different from that in [29], we use the cross-distribution instead of the original dual-vias arrangement to obtain a structural asymmetry that facilitates open stopband suppression. As can be seen from Fig. 5, after adding the open stopband suppression posts, the |S11| is lower than −10 dB at 28 GHz. The lower |S21| in Fig. 5 indicates a higher radiation efficiency.

C. OPTIMIZATION OF THE OPEN STOPBAND SUPPRESSION STRUCTURE

From the parameters in Table 1, it can be seen that the size of inductive posts used to suppress the open stopband is very small. As we know, in consideration of antenna processing restriction, the diameter of inductive post is preferably greater than 0.25 mm, and the minimum spacing of inductive posts is at least 0.2 mm. In the design of antenna with ±35° beam radiation, diameter of the inductive posts r is only 0.15 mm and the lateral distance between two inductive posts u is merely 0.025 mm, which is not realistic for the antenna processing. Therefore, for Ka-band SIW LWA, the method of inserting inductive posts in the waveguide to suppress the open stopband brings challenges to the antenna processing.

In [29], the equivalent circuit analysis of inductive posts for eliminating open stopband is based on a unit cell of the equivalent rectangular waveguide periodic structure. However, for SIW structure as shown in Fig. 6 (a), the metal vias on both sides are used to replace the metal wall of the waveguide. Although they are similar in the performance of transmission characteristics, they are different in terms of equivalent circuit, so the unit cell of SIW structure is analyzed

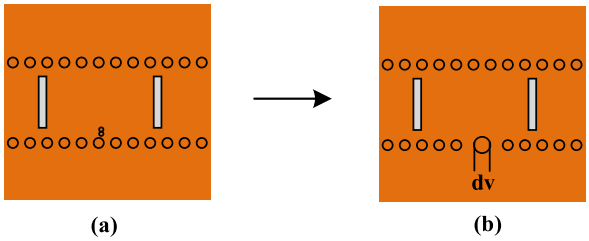

FIGURE 6. Optimization structure of open stopband, (a) original structure, (b) optimized structure.

and further optimized into a new unit cell for suppressing the open stopband.

As we know, the inserted inductive posts and the nearest metal vias of SIW can be seen as two independent shunt inductors, the total inductance of them is smaller than either of them. Therefore, we speculate that reducing the shunt inductance of the SIW periodically can suppress the open stopband. Thus, as shown in Fig. 6 (b), an optimized structure for suppressing open stopband is designed. Instead of adding additional inductive posts, radius of one via in the lateral walls of SIW is enlarged, which causes a sparse distribution of the local vias. Therefore, a smaller inductor value can be expected, and the open stopband can be suppressed.

The simulated S-parameters of the open stopband suppression structure with local sparse vias are shown in Fig. 7. As can be seen, the open stopband is successfully suppressed and a broadband characteristic is obtained, which verifies the effectiveness of the proposed approach. This approach of suppressing open stopband, without inserting additional vias in waveguide, is easy to implement and reduces the fabrication difficulty of Ka-band SIW LWA.

D. INTEGRATION OF ANTENNA ARRAY FOR EXTEDING WAVE COVERAGE

Based on the inherent high-gain feature of leaky-wave antenna, in order to meet the multi-beam and wide coverage requirement of millimeter wave communication, antenna with the capability of beam scanning or beam switching is needed. By the same design procedure, dual-beam antenna elements with radiation beam angles at ±45°, ±55°, ±65° and ±75° are designed. Then together with the ±35° dual-beam antenna, five LWA elements with different beam angles are integrated compactly on one substrate forming a composite planar antenna array, as shown in Fig. 8. By exciting from different feeding ports, the beam switching capability at a certain frequency can be achieved.

As depicted in Fig. 8 (a), the lengths of five LWA elements with diverse beam angles are different. The reason is to make the gain of these antennas comparable, so the slots number of them are designed to be the same. For each antenna, the dominate length of the LWA is chosen to be 14 times of its waveguide length, and total 29 slots are created. Therefore, as indicated in the colorful beam patterns in Fig. 8, when the antenna has a larger beam angle, the length of antenna

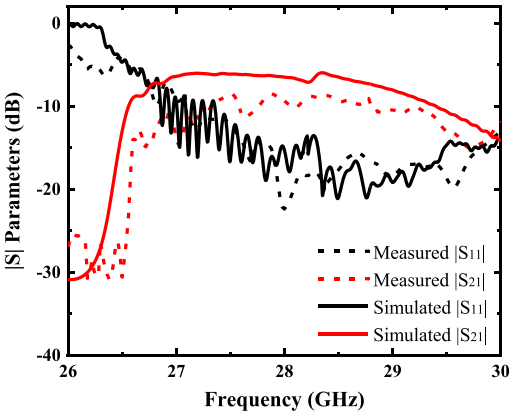

FIGURE 7. S-parameters of the LWAs for ±35° radiation with optimized open stopband suppression structure.

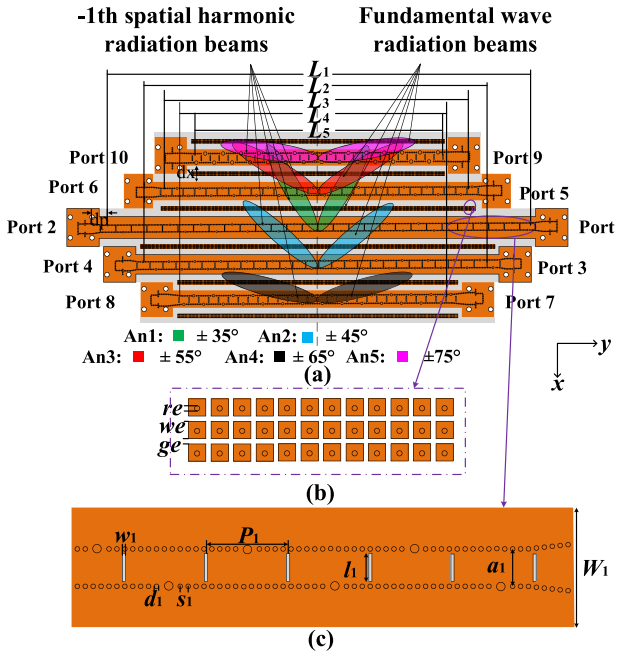

FIGURE 8. Configurations of SIW LWA array, (a) Overall view, (b) EBG structure, (c) detail view of SIW LWA with ±35° radiation beams.

decreases because of its smaller slot period. In order to obtain the structural symmetry aesthetics, these LWAs are arranged according to the law of decreasing the length from middle to sides, and finally form an elliptical-like structure. The middle antenna with radiation beam angles of $\pm 35^{\circ}$ is called An1, the two antennas next to it are named as An2 and An3 with radiation beam angles of $\pm 45^{\circ}$ and $\pm 55^{\circ}$ respectively, and the two outermost antennas are called An4 and An5 with radiation beam angles of $\pm 65^{\circ}$ and $\pm 75^{\circ}$ respectively. The part of detail structure of An1 is shown in Fig. 8 (c).

Table 1 gives the main parameters of antenna elements, where $i = 1, 2, 3, 4, 5$, correspond to An1, An2, An3, An4 and An5 respectively. From Table 1, we can see that the period values P_i satisfy the periodic condition, that is, P_i is greater than P_{mini} and less than P_{maxi}, and ε_{gi} is less than 1. Meanwhile, the values of P_i are all half of the corresponding

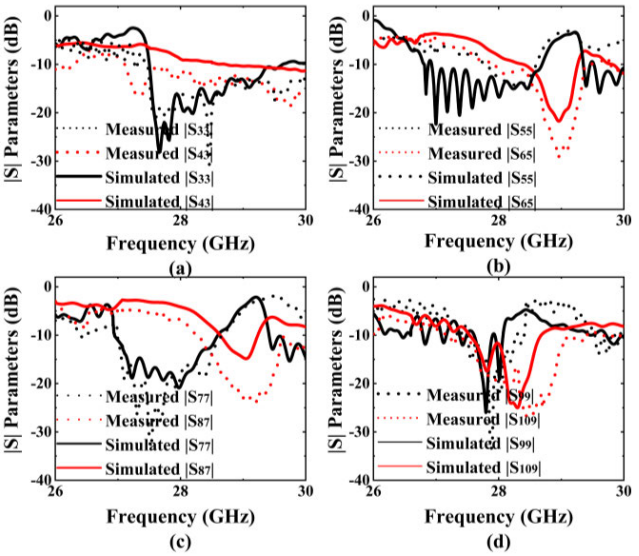

FIGURE 9. Simulated and measured S-parameters of the SIW LWA array with optimized open stopband suppression structure.

waveguide wavelengths, and the *S*-parameters of the SIW LWA array show that the open stopbands for the rest of four elements are suppressed, as illustrated in Fig. 9.

As a leaky-wave antenna array, the mutual-coupling due to the surface wave is an important issue that affects the antenna performance. Surface wave propagates along the antenna aperture and reaches the edges where part of them is reflected and part of them radiates into free space, causing fluctuations in both aperture field distribution and radiation pattern. In this work, the radiation pattern of integrated array will be severely distorted if the surface wave is not suppressed. So, three rows of mushroom-type electromagnetic bandgap (EBG) structures [32] are arranged in between every two elements, as shown in Fig. 8 (b). The patch width is *we*, the spacing between patches is *ge*, and the diameter of the middle vias is *re*, the values are shown in Table 1. By using EBG structure, the mutual coupling is reduced significantly, and the influence of surface wave on radiation pattern is also suppressed.

IV. RESULTS AND DISCUSSION

The proposed SIW LWA array was simulated, fabricated and measured. Fig. 10 shows the fabricated prototype of the SIW LWA array with one port of the middle antenna excited and other ports loaded.

The simulated and measured *S*-parameters of the proposed antenna array are shown Fig. 9, where figures (a) - (d) correspond to LWA elements with beam angles at ±45, ±55, ±65 and ±75 degrees, respectively, the case of beam angles at ±35 degrees are already given in Fig. 7. As shown in Fig. 9, for each antenna element, the measured return loss and insertion loss are basically consistent with the simulated results and the return loss is less than 10 dB at 28 GHz. The measured insertion losses are generally lower than the simulated values, which may be caused by the impedance mismatching of the connectors.

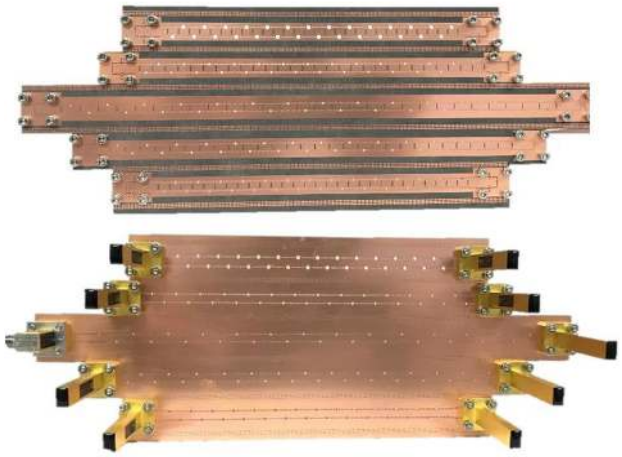

FIGURE 10. Fabricated prototype of the siw lwa array: front view and back view.

Fig. 11 depicts the normalized simulated and measured radiation patterns of the proposed dual-beam antenna array at 28 GHz, when feeding from different ports. The simulated cross-polarization patterns are also given in Fig. 11. As can be seen, the cross-polarization levels are lower than −30 dB at the main beam directions. Moreover, some discrepancies between the simulation and measurement results can be observed, such as the derivation of radiation beams. These errors are mainly caused by the fabrication tolerance in substrate parameters and fabrication process. It should be pointed out that due to the inherent dispersion characteristic of leaky-wave structures, the beam direction of the proposed LWA will change when frequency varies.

Fig.12 demonstrates the simulated and measured gains and simulated radiation efficiencies of the dual-beam antenna array with different beam angles. As can be seen, the simulated gains are all larger than 12 dB, and the differences between the simulated gain and the measured results are less than 3 dB, which is expected. As also shown in this figure, most of the radiation efficiencies are exceed 75%, the lowest one is 56%, which indicates the inherent high efficiency characteristics of the dual harmonic radiation.

V. REALIZATION OF BEAM SWITCHING

The switching network consists of one single-pole double-throw (SPDT) switch, and two single-pole four-throw (SPFT) switches, meanwhile, seven semi-flexible cables are used. as shown in Fig.13, the output ports RF1 and RF2 of SPDT switch control the upper and lower spft switches respectively. meanwhile, the output ports RF1, RF3 and RF4 of the upper spft switch are connected to the three input ports of the antenna, namely port 1, port 3 and port 7. the output ports RF1 and RF2 of the lower spft switch are connected to the rest two input ports of the antenna array, namely port 9 and port 5. therefore, by changing the voltage of these switch chips, the excitation port of the antenna array can be arbitrarily selected to achieve the beam switching capability.

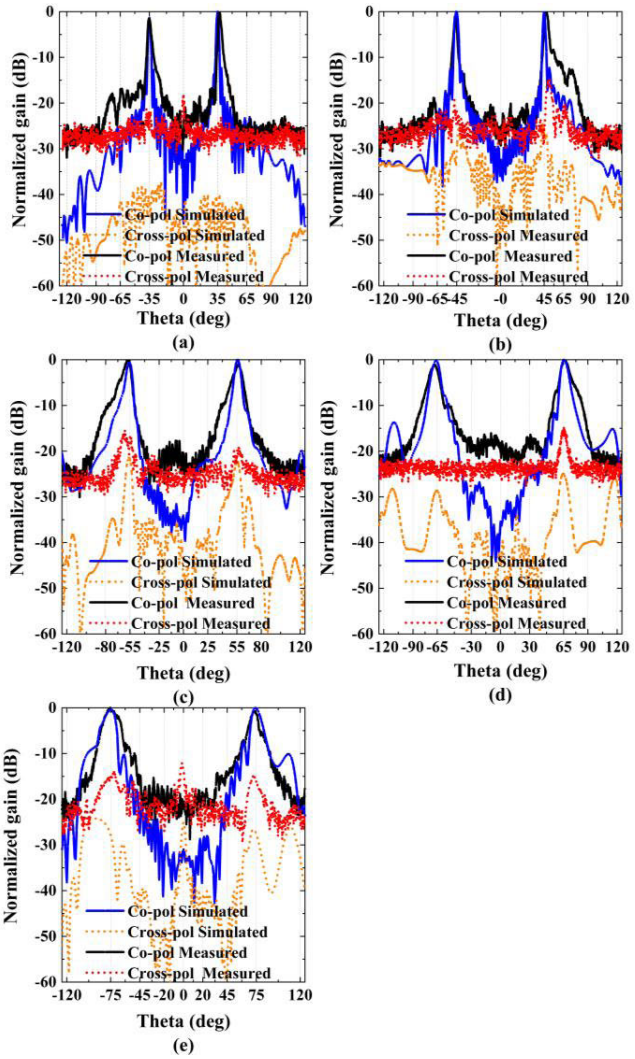

FIGURE 11. Normalized simulated and measured radiation patterns of the proposed antenna array at 28 GHz when feeding from different ports, (a) port 1 of An1, (b) port 3 of An2, (c) port 5 of An3, (d) port 7 of An4, (e) port 9 of An5.

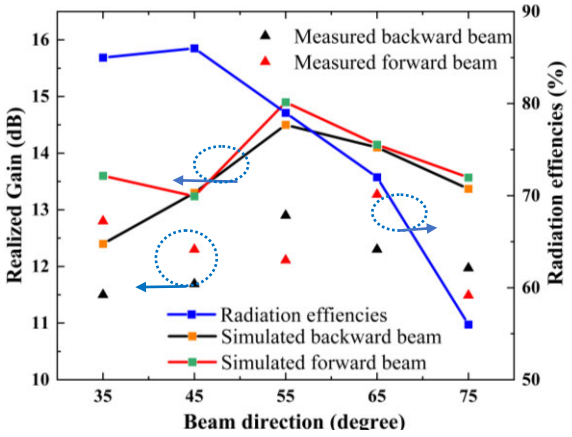

FIGURE 12. Simulated and measured gains, and simulated radiation efficiencies of the LWA array with different beam angles.

The LWA array together with the switch network (on the back side) constitute a voltage-driven beam-switchable

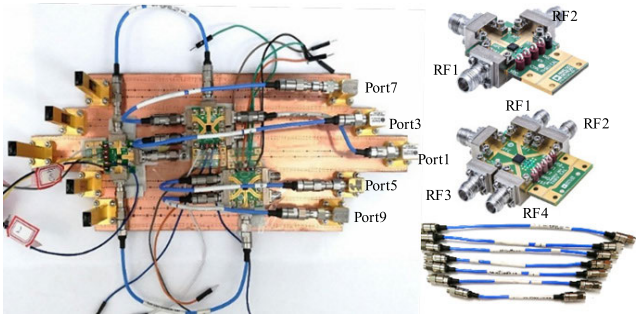

FIGURE 13. Composition of the switch network with the proposed antenna array.

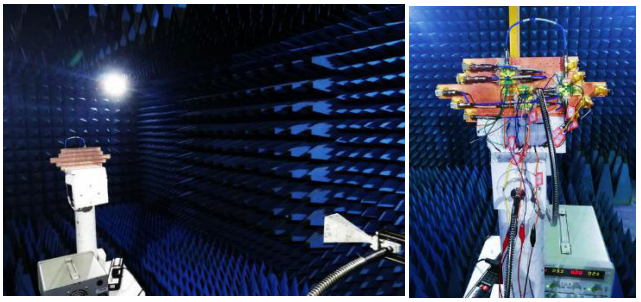

FIGURE 14. Voltage-driven beam-switchable antenna system in measured environment.

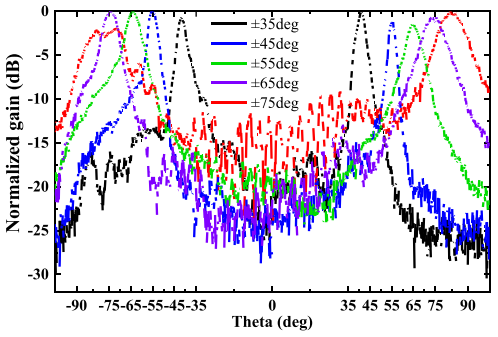

FIGURE 15. Switchable radiation patterns of the antenna array with switches at 28 GHz.

antenna system, which was measured in a microwave anechoic chamber, as shown in Fig.14. the measured normalized radiation patterns of the antenna system at 28 GHz are plotted in Fig. 15. It is observed that the measured beam angles are basically consistent with those of antenna array without switches as shown in Fig. 11, excepting some slight shift of the beam angles.

As shown in Table 2, by making comparison between this work and other relative references, some obvious superiorities of the proposed design can be summarized: 1) it is capable of fixed-frequency beam scanning while other available dual-beam designs based on SIW structure cannot; 2) the beam scanning range is wider than other available dual-beam antennas; 3) has a feasible port switching scheme than other available dual-beam antennas.

TABLE 2. Comparison between the proposed and the relative symmetrical dual beam antennas.

Ref.	Antenna type	Frequency (GHz)	Scanning range (left/right beam)	Gain	Feasible port switching
[17]	Dielectric Grating	57-63	-20°- -32°/22°-28°	23.3/25.1 dBi	-
[20]	SIW	13	-	2.5/7 dB	-
[21]	SIW	8.5-13.3	74°/74°	-	-
[22]	Microstrip	7	234°-282°/78°-126°	-	No
[23]	Coplanar Waveguide	5.8	-	11.9/11.9 dB	No
This Work	SIW	28	-35°- -75°/35°-75°	14.3/15 dB	Yes

VI. CONCLUSION

In this work, a novel design of antenna array for fixed-frequency dual-beam switching is proposed and fabricated, which contains five integrated LWA elements with different dual-beam angles. Each antenna works on fundamental wave and -1th spatial harmonic wave simultaneously and excites two symmetrical radiation beams in forward and backward direction respectively. A method of suppressing open stopband is put forward, which is simple and can be used in Ka-band for reducing the fabrication difficulty. Three voltage-driven CSW-RF switches are integrated on the back side of the antenna array to form a miniature input ports switching system. By controlling voltage, the CSW-RF switches can selectively excite different input ports to achieve different dual-beam angles at a fixed frequency. The measured results validate the feasibility of the proposed design. However, some disadvantages still exist in this design, such as large loss of the switches, the effect of open stopband has not been suppressed completely and sidelobe level is still high. These limitations will be further studied in future work.

REFERENCES

[1] A. A. Oliner and D. R. Jackson, "Leaky-wave antennas," in *Antenna Engineering Handbook*, J. Volakis, Ed., 4th ed. New York, NY, USA: McGraw-Hill, 2007, ch. 10.

[2] D. Deslandes and K. Wu, "Accurate modeling, wave mechanisms, and design considerations of a substrate integrated waveguide," *IEEE Trans. Microw. Theory Techn.*, vol. 54, no. 6, pp. 2516–2526, Jun. 2006.

[3] S.-L. Chen, D. K. Karmokar, Z. Li, P.-Y. Qin, R. W. Ziolkowski, and Y. J. Guo, "Circular-polarized substrate-integrated-waveguide leaky-wave antenna with wide-angle and consistent-gain continuous beam scanning," *IEEE Trans. Antennas Propag.*, vol. 67, no. 7, pp. 4418–4428, Jul. 2019.

[4] Y. R. Ding and Y. J. Cheng, "Ku/Ka dual-band dual-polarized shared-aperture beam-scanning antenna array with high isolation," *IEEE Trans. Antennas Propag.*, vol. 67, no. 4, pp. 2413–2422, Apr. 2019.

[5] Y.-L. Lyu, F.-Y. Meng, G.-H. Yang, D. Erni, Q. Wu, and K. Wu, "Periodic SIW leaky-wave antenna with large circularly polarized beam scanning range," *IEEE Antennas Wireless Propag. Lett.*, vol. 16, pp. 2493–2496, 2017.

[6] Y. Geng, J. Wang, Y. Li, Z. Li, M. Chen, and Z. Zhang, "Radiation pattern-reconfigurable leaky-wave antenna for fixed-frequency beam steering based on substrate-integrated waveguide," *IEEE Antennas Wireless Propag. Lett.*, vol. 18, no. 2, pp. 387–391, Feb. 2019.

[7] Z. Li, Y. J. Guo, S.-L. Chen, and J. Wang, "A period-reconfigurable leaky-wave antenna with fixed-frequency and wide-angle beam scanning," *IEEE Trans. Antennas Propag.*, vol. 67, no. 6, pp. 3720–3732, Jun. 2019.

[8] A. Iftikhar, M. Ur-Rehman, M. F. Shafique, U. Farooq, M. S. Khan, S. M. Asif, A. Fida, B. Ijaz, M. N. Rafique, and M. J. Mughal, "Planar SIW leaky wave antenna with electronically reconfigurable E-and H-plane scanning," *IEEE Access*, vol. 7, pp. 171206–171213, 2019.
[9] A. Suntives and S. V. Hum, "A fixed-frequency beam-steerable half-mode substrate integrated waveguide leaky-wave antenna," *IEEE Trans. Antennas Propag.*, vol. 60, no. 5, pp. 2540–2544, May 2012.
[10] C. Luxey and J.-M. Laheurte, "Simple design of dual-beam leaky-wave antennas in microstrips," *IEE Proc., Microw. Antennas Propag.*, vol. 144, no. 6, pp. 397–402, Dec. 1997.
[11] C. Chen, Y. Guo, and H. Wang, "Wideband symmetrical cross-shaped probe dual-beam microstrip patch antenna," *IEEE Antennas Wireless Propag. Lett.*, vol. 14, pp. 622–625, 2015.
[12] C.-C. Hu, C. Jsu, and J.-J. Wu, "An aperture-coupled linear microstrip leaky-wave antenna array with two-dimensional dual-beam scanning capability," *IEEE Trans. Antennas Propag.*, vol. 48, no. 6, pp. 909–913, Jun. 2000.
[13] Q. Liu, S.-S. Qi, Q. Yin, and W. Wu, "Frequency-scanning dual-beam parallel-plate waveguide continuous transverse stub antenna array with sidelobe suppression," *IEEE Antennas Wireless Propag. Lett.*, vol. 17, no. 7, pp. 1228–1232, Jul. 2018.
[14] W. Yang, L. Gu, W. Che, Q. Meng, Q. Xue, and C. Wan, "A novel steerable dual-beam metasurface antenna based on controllable feeding mechanism," *IEEE Trans. Antennas Propag.*, vol. 67, no. 2, pp. 784–793, Feb. 2019.
[15] T.-L. Chen and Y.-D. Lin, "Dual-beam microstrip leaky-wave array excited by aperture-coupling method," *IEEE Trans. Antennas Propag.*, vol. 51, no. 9, pp. 2496–2498, Sep. 2003.
[16] Z. L. Ma and L. J. Jiang, "One-dimensional triple periodic dual-beam microstrip leaky-wave antenna," *IEEE Antennas Wireless Propag. Lett.*, vol. 14, pp. 390–393, 2015.
[17] Z. L. Ma, K. B. Ng, C. H. Chan, and L. J. Jiang, "A novel supercell-based dielectric grating dual-beam leaky-wave antenna for 60-GHz applications," *IEEE Trans. Antennas Propag.*, vol. 64, no. 12, pp. 5521–5526, Dec. 2016.
[18] C.-J. Wang, C. Jou, and J.-J. Wu, "A novel two-beam scanning active leaky-wave antenna," *IEEE Trans. Antennas Propag.*, vol. 47, no. 8, pp. 1314–1317, Aug. 1999.
[19] C.-J. Wang, "Active dual-beam leaky-wave antenna with asymmetrically scanning capability," *Electron. Lett.*, vol. 37, no. 11, pp. 672–673, May 2001.
[20] M. Garcia-Vigueras, M. Esquius-Morote, J. Perruisseau-Carrier, and J. R. Mosig, "Dual-beam radiation from ID leaky-wave antennas," in *Proc. 8th Eur. Conf. Antennas Propag. (EuCAP)*, Apr. 2014, pp. 1447–1450.
[21] R. Shaw, A. A. Khan, and M. K. Mandal, "Dual-beam substrate integrated waveguide periodic leaky-wave antenna," in *Proc. Int. Conf. Microw. Photon. (ICMAP)*, Dhanbad, India, Dec. 2015, pp. 1–2.
[22] Y. Li, Q. Xue, E. K.-N. Yung, and Y. Long, "Fixed-frequency dual-beam scanning microstrip leaky wave antenna," *IEEE Antennas Wireless Propag. Lett.*, vol. 6, pp. 444–446, 2007.
[23] P. Liu, Z. Zhang, Y. Li, and Z. Feng, "A dual-beam eight-element antenna array with compact CPWG crossover structure," *IEEE Antennas Wireless Propag. Lett.*, vol. 16, pp. 1269–1272, 2017.
[24] D. R. Jackson, C. Caloz, and T. Itoh, "Leaky-wave antennas," *Proc. IEEE*, vol. 100, no. 7, pp. 2194–2206, Jul. 2012.
[25] J. Wang, Y. Geng, C. Zhang, and X. Huo, "Radiation characteristic of the periodic leaky wave structure and its application to leaky wave antenna design," in *Proc. Asia–Pacific Microw. Conf. (APMC)*, Nanjing, China, Dec. 2015, p. 1.
[26] Y. Geng, J. Wang, Y. Li, Z. Li, M. Chen, and Z. Zhang, "Leaky-wave antenna array with a power-recycling feeding network for radiation efficiency improvement," *IEEE Trans. Antennas Propag.*, vol. 65, no. 5, pp. 2689–2694, May 2017.
[27] Y. Li and K.-M. Luk, "A broadband V-band rectangular waveguide to substrate integrated waveguide transition," *IEEE Microw. Wireless Compon. Lett.*, vol. 24, no. 9, pp. 590–592, Sep. 2014.
[28] F. Xu and K. Wu, "Guided-wave and leakage characteristics of substrate integrated waveguide," *IEEE Trans. Microw. Theory Techn.*, vol. 53, no. 1, pp. 66–73, Jan. 2005.
[29] W. Zhou, J. Liu, and Y. Long, "Investigation of shorting vias for suppressing the open stopband in an SIW periodic leaky-wave structure," *IEEE Trans. Microw. Theory Techn.*, vol. 66, no. 6, pp. 2936–2945, Jun. 2018.
[30] R. Shaw and M. K. Mandal, "Broadside scanning asymmetric SIW LWA with consistent gain and reduced sidelobe," *IEEE Trans. Antennas Propag.*, vol. 67, no. 2, pp. 823–833, Feb. 2019.
[31] R. Ranjan and J. Ghosh, "SIW-based leaky-wave antenna supporting wide range of beam scanning through broadside," *IEEE Antennas Wireless Propag. Lett.*, vol. 18, no. 4, pp. 606–610, Apr. 2019.
[32] S. Ebadi and A. Semnani, "Mutual coupling reduction in waveguide-slot-array antennas using electromagnetic bandgap (EBG) structures," *IEEE Antennas Propag. Mag.*, vol. 56, no. 3, pp. 68–79, Jun. 2014.

XIAOWEN LI was born in Shandong, China, in 1992. She received the B.E. degree from the School of Opto-Electronic Information Science and Technology, Yantai University, China, in 2015. She is currently pursuing the Ph.D. degree with the Institute of Lightwave Technology, Beijing Jiaotong University.

Her research fields are leaky-wave antennas and array.

JUNHONG WANG (Senior Member, IEEE) was born in Jiangsu, China, in 1965. He received the B.S. and M.S. degrees in electrical engineering from the University of Electronic Science and Technology of China, Chengdu, China, in 1988 and 1991, respectively, and the Ph.D. degree in electrical engineering from Southwest Jiaotong University, Chengdu, in 1994. In 1995, he joined as a Faculty with the Department of Electrical Engineering, Beijing Jiaotong University, Beijing, China, where he became a Professor, in 1999. From January 1999 to June 2000, he was a Research Associate with the Department of Electric Engineering, City University of Hong Kong, Hong Kong. From July 2002 to July 2003, he was a Research Scientist with Temasek Laboratories, National University of Singapore, Singapore. He is currently with the Key Laboratory of all Optical Network and Advanced Telecommunication Network, Ministry of Education of China, Beijing Jiaotong Univeristy, where he is also with the Institute of Lightwave Technology. His research interests include numerical methods, antennas, scattering, and leaky wave structures.

ZHENG LI (Member, IEEE) received the B.S. degree in physics and the Ph.D. degree in electrical engineering from Beijing Jiaotong University, Beijing, China, in 2006 and 2012, respectively. From 2008 to 2009, he was a Visiting Student with Pennsylvania State University, State College, PA, USA. From 2017 to 2018, he was a Visiting Professor with the University of Technology Sydney, Ultimo, NSW, Australia.

In 2012, he joined the faculty of the Department of Electrical Engineering, Beijing Jiaotong University, where he became an Associate Professor, in 2015. His research interests include leaky-wave antennas and periodic structures.

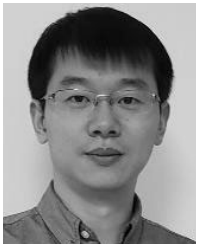

YUJIAN LI (Member, IEEE) was born in Hunan, China, in 1987. He received the B.S. and M.S. degrees in communications engineering from Beijing Jiaotong University, Beijing, China, in 2009 and 2012, respectively, and the Ph.D. degree in electronic engineering from the City University of Hong Kong, in 2015.

In 2015, he joined the Institute of Lightwave Technology, Beijing Jiaotong University, where he is currently a Full Professor with the School of Electronic and Information Engineering. His current research interests include millimeter wave antennas, base station antennas, and leaky wave structures.

Dr. Li was awarded the Outstanding Research Thesis Award from the City University of Hong Kong, in 2015. He received the Best Paper Award at the 2015 IEEE Asia-Pacific Conference on Antennas and Propagation (APCAP), the Best Student Paper at 2013 National Conference on Antennas, and the Best Student Paper Award (Second Prize) at the 2013 IEEE International Workshop on Electromagnetics (iWEM). He was selected as a Finalist in the Student Paper Contest of the 2015 IEEE AP-S Symposium on Antennas and Propagation (APS). He has served as a Reviewer for the IEEE TRANSACTIONS ON ANTENNAS AND PROPAGATION, the IEEE ANTENNAS AND WIRELESS PROPAGATION LETTERS, and the *IET Microwaves, Antennas & Propagation*.

MEIE CHEN received the B.S. degree in information and telecommunication engineering and the Ph.D. degree in electromagnetic and microwave technology from Beijing Jiaotong University, Beijing, China, in 2003 and 2009, respectively.

She is currently a Lecture with the Institute of Lightwave Technology, Beijing Jiaotong University. Her research interests include antenna theory and technology, metasurface, and RCS reduction technique.

ZHAN ZHANG received the B.S degree in electronics and communications engineering from Jilin University, China, in 2002, and the Ph.D. degree in electrical engineering from Nanyang Technological University, Singapore, in 2010. She joined the Faculty of the School of Electronics and Information Engineering, Beijing Jiaotong University, Beijing, China, in 2010, where she is currently an Associate Professor. Her current research interests include metamaterial-based antenna design and transformation optics.